

**COUPLED MAGNETO-ELASTIC AND
ELECTRO-ELASTIC EFFECTS IN RODS**

DARIUS DIOGO BARRETO



**DEPARTMENT OF APPLIED MECHANICS
INDIAN INSTITUTE OF TECHNOLOGY DELHI
SEPTEMBER 2022**

© Indian Institute of Technology Delhi (IITD), New Delhi, 2022

COUPLED MAGNETO-ELASTIC AND ELECTRO-ELASTIC EFFECTS IN RODS

by

DARIUS DIOGO BARRETO

Department of Applied Mechanics

Submitted
in fulfillment of the requirements of the degree of Doctor of Philosophy
to the



INDIAN INSTITUTE OF TECHNOLOGY DELHI
SEPTEMBER 2022

*Dedicated To
My Parents*

Certificate

This is to certify that the thesis entitled “**Coupled magneto-elastic and electro-elastic effects in rods**” is being submitted by **Mr. Darius Diogo Barreto** to the Indian Institute of Technology Delhi for the award of the degree of **Doctor of Philosophy**, is a record of bonafide research carried out by him under my supervision. The thesis in my opinion, is worthy of consideration in accordance with the rules and regulations of the Institute. To the best of my knowledge, the results embodied in this thesis have not been submitted to any other University or Institute for the award of any other degree or diploma.

Prof. Ajeet Kumar
Associate Professor
Department of Applied Mechanics
Indian Institute of Technology Delhi
New Delhi-110016
India

Acknowledgements

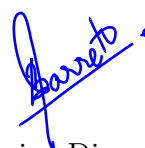
I want to express my sincere gratitude to Professor Ajeet Kumar, my research advisor, for his guidance and support throughout my graduate study. He always motivated me to pursue fundamental research in solid mechanics. This dissertation would not have reached its final stage without his efforts and dedication. I am grateful to him for sharing his immense knowledge through the countless meetings and discussions, which helped me understand this work better. In the past six years, I received guidance in just about every aspect of my life from him. He was always available to discuss essential matters regarding my research and even my well-being. I also learned heavily from the courses he taught me, i.e., Applied Elasticity, Advanced Solid mechanics and Computational Mechanics, Advanced Finite Element Method. I would also like to express my sincere thanks to Prof. Sushma Santapuri, with whom I collaborated in 2017. She guided me on magnetoelasticity during the early stage of my Ph.D. Her guidance has played a significant role in the development of the work presented in Chapter 2.

I would also like to express my gratitude to my student research committee members: Professor Sushma Santapuri, Professor Prof. M.K Singha, and Professor J.P. Singh, for their willingness to serve on my committee. I am highly grateful to them for finding the time, despite their busy schedule, to read through my dissertation in greater detail and for giving me many valuable suggestions for improvement. I also express my sincere thanks to other faculty members of IIT Delhi for their constant support.

I am incredibly grateful to all my labmates and colleagues: Prof. Prakhar Gupta, Dr. Raushan Singh, Dr. Smriti, Mohit Garg, Intaf Alam, Manoj Shikhar, Pulkit Singhal, Roushan Kumar, and Vinayak their valuable suggestions and help. The lengthy discussions, especially with Smriti, Mohit, and Intaf, have helped me improve my understanding of the various concepts. I owe my deepest gratitude to my colleague Prof. Prakhar Gupta, who has been a wonderful friend and a great mentor since the beginning of my Ph.D. journey. I cannot thank him enough for his support during the utmost need.

Special thanks are also due to my wife Divine Savia Pereira for her many sacrifices, understanding, friendship, and love. She stood beside me through good and bad times. Without her, I could never have come this far. She encouraged me to pursue Ph.D. despite the constraints and provided emotional support throughout this journey. I would also like to thank my parents and siblings, who supported me unconditionally. They have always trusted and encouraged me in my endeavors. This dissertation is a culmination of their support, time, and energy put into me.

I want to thank the Applied Mechanics Department of IIT Delhi for giving me this opportunity for my graduate studies. I feel fortunate to be a part of the IIT Delhi community. Finally, I would like to thank the Lord for guiding and blessing me throughout this journey.



Darius Diogo Barreto

Abstract

Over the past few years, there has been a significant increase in the popularity of smart materials. Magneto and electro-elastic polymers are one of the most widely used polymers, which make them prominent candidates in biomedical engineering (e.g., tissue engineering, drug delivery systems), soft matter engineering (e.g., soft robotics), design of smart structures and systems with dynamic properties. To further improve the utility of these materials in device design, it is essential to develop mathematical models that can describe their coupled nonlinear characteristics. Many of the works to model slender magneto and electro-elastic structures focus on using the classical beam theories such as the Euler-Bernoulli and Timoshenko beam theories. However, these theories are geometrically linear, which can model only small rotation of the beam's cross-section. On the other hand, the theory of rods is nonlinear and geometrically exact, allowing large rotation of the cross-section which, in turn, also requires nonlinear constitutive relations when the induced curvature and twist are large enough. This thesis aims to develop nonlinear magneto/electro-elastic theories for rods and tubes.

The first part of this thesis focuses on developing an axisymmetric and axially homogeneous variational formulation to model coupled extension-torsion-inflation deformation in compressible magnetoelastic thin tubes with helical magnetic anisotropy in the presence of azimuthal and axial magnetic fields. The tube's material is assumed to have a preferred magnetization direction which lies in the radial plane but at an angle from the tube's axial direction - this imparts helical magnetic anisotropy to the tube. The governing differential equations necessary to solve the above deformation problem are obtained, which are shown to reduce to a set of nonlinear algebraic equations in the thin tube limit. Hence analytical expressions can be obtained in terms of the applied magnetic field, preferred magnetization direction, and magnetoelastic constants, which tells how these parameters can be tuned to generate unusual coupled deformations such as negative Poisson's effect.

The second part of this thesis proposes a theory for finite and spatial elastic deformation of rods under the influence of arbitrary magnetic field and boundary conditions. The rod is modeled as a Kirchhoff rod. It is assumed to have a uniformly distributed array of uniaxial spheroidal paramagnetic inclusions embedded in it, all pointing in the same direction in the undeformed state. The governing equations of the magnetoelastic rod have been derived which are further non-dimensionalized and linearized to investigate buckling in such rods. Analytical expressions for the onset of buckling from the rod's trivial state are obtained in terms of loading parameters (applied magnetic field, axial load, torque) as well as geometric (inclusion orientation in the undeformed state) and material (ratio of bending and torsional stiffnesses) parameters for different combinations of boundary conditions. The buckled shape of the rod at the onset of buckling is also examined.

Finally, a theory to model deformation in electroelastic slender bodies also incorporating the free space energy has been proposed. The electric polarization of most electroelastic polymers is relatively weak compared to piezoelectric materials. Therefore, while modeling electroelastic polymers, the contribution of free space energy may be significant. In this context, a one-dimensional electroelastic rod theory also incorporating the free space energy has been proposed. The rod is modeled as a Kirchhoff rod. The governing equations have been derived by doing the balance of all the forces and moments (arising from both mechanical and electrical sources) that act on an arbitrary segment of the electroelastic rod. Furthermore, the governing equations for the electric potential parameters are derived by multiplying the Maxwell equation for electric displacement with cross-sectional coordinates and further integrating in the cross-section. On non-dimensionalizing, the leading order contributions of the electric terms in them are identified. Additionally, using the method of matched asymptotic expansions, asymptotically accurate algebraic equations have been derived for the unknown free space electric field directly from the boundary integral representation of the Laplace equation for the electric potential in the free space. The effect of free space on the deformation field inside the electroelastic body is numerically shown to be significant thus highlighting the importance of including the free space energy which is largely neglected in the literature.

सार

पिछले कुछ वर्षों में, स्मार्ट सामग्री की लोकप्रियता में उल्लेखनीय वृद्धि हुई है। मैग्नेटो और इलेक्ट्रो-इलास्टिक पॉलिमर सबसे व्यापक रूप से उपयोग किए जाने वाले पॉलिमर में से एक हैं, जो उन्हें बायोमेडिकल इंजीनियरिंग (जैसे, टिशू इंजीनियरिंग, ड्रग डिलीवरी सिस्टम), सॉफ्ट मैटर इंजीनियरिंग (जैसे, सॉफ्ट रोबोटिक्स), स्मार्ट संरचनाओं और सिस्टम के डिजाइन में प्रमुख उम्मीदवार बनाते हैं। गतिशील गुणों के साथ। डिवाइस डिजाइन में इन सामग्रियों की उपयोगिता को और बेहतर बनाने के लिए, गणितीय मॉडल विकसित करना आवश्यक है जो उनकी युग्मित गैर-रेखीय विशेषताओं का वर्णन कर सकें। पतला मैग्नेटो और इलेक्ट्रो-इलास्टिक संरचनाओं को मॉडल करने के लिए कई काम शास्त्रीय बीम सिद्धांतों जैसे कि यूलर-बर्नौली और टिमोशेंको बीम सिद्धांतों का उपयोग करने पर ध्यान केंद्रित करते हैं। हालांकि, ये सिद्धांत ज्यामितीय रूप से रैखिक हैं, जो बीम के क्रॉस-सेक्शन के केवल छोटे रोटेशन को मॉडल कर सकते हैं। दूसरी ओर, छड़ का सिद्धांत गैर-रेखीय और ज्यामितीय रूप से सटीक है, जिससे क्रॉस-सेक्शन के बड़े रोटेशन की अनुमति मिलती है, जिसके बदले में, गैर-रेखीय संवैधानिक संबंधों की भी आवश्यकता होती है, जब प्रेरित वक्रता और मोड़ काफी बड़े होते हैं। इस थीसिस का उद्देश्य छड़ और ट्यूबों के लिए नॉनलाइनियर मैग्नेटो/इलेक्ट्रो-इलास्टिक सिद्धांतों को विकसित करना है।

इस थीसिस का पहला भाग अजीमथल और अक्षीय चुंबकीय क्षेत्रों की उपस्थिति में पेचदार चुंबकीय अनिसोट्रॉपी के साथ संपीडित मैग्नेटोएलास्टिक पतली ट्यूबों में मॉडल युग्मित विस्तार-मरोड़-मुद्रास्फीति विरूपण के लिए एक अक्षीय और अक्षीय रूप से समरूप रूपांतर विकसित करने पर केंद्रित है। ट्यूब की सामग्री को एक पसंदीदा चुंबकीयकरण दिशा माना जाता है जो रेडियल विमान में स्थित होती है लेकिन ट्यूब की अक्षीय दिशा से कोण पर होती है - यह ट्यूब को पेचदार चुंबकीय अनिसोट्रॉपी प्रदान करती है। उपरोक्त विकृति समस्या को हल करने के लिए आवश्यक शासी अंतर समीकरण प्राप्त किए जाते हैं, जो पतली ट्यूब सीमा में गैर-रेखीय बीजीय समीकरणों के एक सेट को कम करने के लिए दिखाए जाते हैं। इसलिए विश्लेषणात्मक अभिव्यक्तियों को लागू चुंबकीय क्षेत्र, पसंदीदा चुंबकीयकरण दिशा और मैग्नेटोएलास्टिक स्थिरांक के संदर्भ में प्राप्त

किया जा सकता है, जो बताता है कि इन मापदंडों को असामान्य युग्मित विकृतियों जैसे कि नकारात्मक पॉइसन के प्रभाव को उत्पन्न करने के लिए कैसे ट्यून किया जा सकता है।

इस थीसिस का दूसरा भाग मनमाने चुंबकीय क्षेत्र और सीमा स्थितियों के प्रभाव में छड़ के परिमित और स्थानिक लोचदार विरूपण के लिए एक सिद्धांत का प्रस्ताव करता है। रॉड को किरचॉफ रॉड के रूप में तैयार किया गया है। यह माना जाता है कि इसमें एक समान रूप से वितरित एक अक्षीय गोलाकार पैरामैग्नेटिक समावेशन है, जो सभी विकृत अवस्था में एक ही दिशा में इंगित करते हैं। मैग्नेटोएलास्टिक रॉड के शासी समीकरणों को व्युत्पन्न किया गया है जो आगे गैर-आयामी हैं और ऐसी छड़ों में बकलिंग की जांच करने के लिए रखे हैं। रॉड की तुच्छ अवस्था से बकलिंग की शुरुआत के लिए विश्लेषणात्मक अभिव्यक्तियाँ लोडिंग मापदंडों (लागू चुंबकीय क्षेत्र, अक्षीय भार, टोक) के साथ-साथ ज्यामितीय (अविकसित अवस्था में समावेश अभिविन्यास) और सामग्री (झुकने और मरोड़ने का अनुपात) के संदर्भ में प्राप्त की जाती हैं।) सीमा स्थितियों के विभिन्न संयोजनों के लिए पैरामीटर। बकलिंग की शुरुआत में रॉड के मुड़े हुए आकार की भी जांच की जाती है।

अंत में, इलेक्ट्रोएलास्टिक पतला निकायों में मॉडल विरूपण के सिद्धांत को भी मुक्त अंतरिक्ष ऊर्जा को शामिल करने का प्रस्ताव दिया गया है। अधिकांश इलेक्ट्रोइलास्टिक पॉलिमर का विद्युत ध्रुवीकरण पीजोइलेक्ट्रिक सामग्री की तुलना में अपेक्षाकृत कमजोर है। इसलिए, इलेक्ट्रोइलास्टिक पॉलिमर की मॉडलिंग करते समय, मुक्त अंतरिक्ष ऊर्जा का योगदान महत्वपूर्ण हो सकता है। इस संदर्भ में, मुक्त अंतरिक्ष ऊर्जा को शामिल करते हुए एक आयामी इलेक्ट्रोइलास्टिक रॉड सिद्धांत प्रस्तावित किया गया है। रॉड को किरचॉफ रॉड के रूप में तैयार किया गया है। शासी समीकरण सभी बलों और क्षणों (यांत्रिक और विद्युत दोनों स्रोतों से उत्पन्न) के संतुलन को करके प्राप्त किए गए हैं जो इलेक्ट्रोएलास्टिक रॉड के एक मनमाना खंड पर कार्य करते हैं। इसके अलावा, विद्युत संभावित मापदंडों के लिए शासी समीकरण क्रॉस-अनुभागीय निर्देशांक के साथ विद्युत विस्थापन के लिए मैक्सवेल समीकरण को गुणा करके और क्रॉस-सेक्शन में आगे एकीकृत करके प्राप्त किए जाते हैं। गैर-आयामीकरण पर, उनमें विद्युत शर्तों के अग्रणी क्रम योगदान की पहचान की जाती है। इसके अतिरिक्त, मिलान किए गए स्पर्शान्मुख विस्तारों की विधि का उपयोग करते

हूए, अज्ञात मुक्त स्थान विद्युत क्षेत्र के लिए स्पर्शोन्मुख रूप से सटीक बीजगणितीय समीकरण सीधे मुक्त स्थान में विद्युत क्षमता के लिए लाप्लास समीकरण के सीमा अभिन्न प्रतिनिधित्व से प्राप्त किए गए हैं। इलेक्ट्रोइलास्टिक बॉडी के अंदर विरूपण क्षेत्र पर मुक्त स्थान का प्रभाव संख्यात्मक रूप से महत्वपूर्ण दिखाया गया है, इस प्रकार मुक्त अंतरिक्ष ऊर्जा को शामिल करने के महत्व पर प्रकाश डाला गया है जिसे साहित्य में काफी हद तक उपेक्षित किया गया है।

Contents

Certificate	i
Acknowledgements	ii
Abstract	iii
List of Figures	xiii
List of Tables	xiv
1 Introduction	1
1.1 Coupled deformation in helically reinforced magnetoelastic tubes	1
1.2 A magetoelastic theory for Kirchhoff rods having uniformly distributed paramagnetic inclusions	3
1.3 A one dimensional electroelastic Kirchhoff rod theory incorporating free space enegy	5
1.4 Objectives and organization of the thesis	6
2 Coupled extension-torsion-inflation deformation in compressible magnetoelastic thin tubes with helical magnetic anisotropy	8
2.1 A brief note on magnetoelasticity	9
2.1.1 Maxwell equation for magnetic field	10
2.1.2 Linear and angular momentum balance for mechanical deformation	10
2.1.3 Coupled constitutive equations	11
2.1.4 Variational formulation	11
2.2 Axisymmetric and axially homogeneous formulation	11
2.2.1 Magnetic field solution	13
2.2.2 A variational formulation to obtain in-plane deformation	15
2.3 Expressions of induced axial force, twisting moment, internal pressure, azimuthal and axial magnetization flux	16
2.4 Thin tube approximation	18
2.5 Effect of small magnetic field parameters (ζ and η) on coupled deformation in thin tubes	19
2.5.1 Effective Poisson's ratio of magnetoelastic tubes	21
2.5.2 Overwinding/unwinding characteristic of magnetoelastic tubes	23
2.6 Coupled deformation in finitely stretched tubes	25
2.6.1 Induced pressure vs. imposed inflation	25

2.6.2	Extension-inflation coupling	27
2.6.3	Extension-torsion coupling	27
2.7	Summary	29
3	A magnetoelastic theory for Kirchhoff rods having uniformly distributed paramagnetic inclusions and its buckling	30
3.1	Introduction	30
3.2	A brief description of a Kirchhoff rod	31
3.3	Magnetoelastic rods	32
3.3.1	Magnetic energy of a single inclusion	32
3.3.2	Total energy of a magnetoelastic rod and its equations of equilibrium	34
3.3.3	Interpretation of governing equations	36
3.4	Non-dimensional form of governing equations and its linearization	38
3.5	Magnetic field perpendicular to undeformed inclusion orientation	40
3.5.1	Clamped-Free boundary condition	42
3.5.2	Pinned-Pinned boundary condition	43
3.5.3	Clamped-Pinned boundary condition	43
3.5.4	Clamped-Clamped boundary condition	44
3.5.5	Specific cases of $\phi = 0$ and $\phi = \pi/2$	45
3.5.6	Buckling condition when only magnetic field is present	46
3.5.7	Graphical representation of buckling equations	48
3.6	Magnetic field parallel to undeformed inclusion orientation	48
3.6.1	specific cases of $\phi = 0$ and $\phi = \pi/2$	51
3.6.2	Presence of only magnetic field	53
3.6.3	Graphical representation of buckling equations	53
3.7	Buckling in the presence of magnetic field, axial load and twisting moment	54
3.7.1	Case (i): Axially aligned undeformed inclusions with perpendicular magnetic field	55
3.7.2	Case (ii): Axially aligned undeformed inclusions and magnetic field	60
3.7.3	Case (iii): Axial magnetic field and undeformed inclusions in the cross-sectional plane	61
3.8	Comparison with existing literature	64
3.9	Summary	65
4	A one-dimensional electroelastic Kirchhoff rod theory also incorporating the free space energy	67
4.1	A brief overview of the three-dimensional theory of electroelasticity	67
4.1.1	Maxwell equation for electric field	68
4.1.2	Linear and angular momentum balance for mechanical deformation	69
4.1.3	Boundary integral equation for the flux variable q	70
4.2	Derivation of the electroelastic Kirchhoff rod theory	71
4.2.1	Kinematics	71
4.2.2	Linear and angular momentum balance	72
4.3	Equations for the electric potential parameters	76
4.4	Leading-order contribution of electric terms in governing equations	78
4.5	Electroelastic constitutive equations	82

4.6	Derivation of equations for the Fourier coefficients of flux variable q . . .	84
4.6.1	Outer region	85
4.6.2	Inner region	85
4.6.3	Common part	86
4.6.4	Composite representation of the boundary integral equation . . .	87
4.7	Complete set of governing equations	91
4.8	Removing singularity from the slender body equation	95
4.9	Numerical Implementation	95
4.9.1	Nonlinear isotropic electroelastic polymer model	96
4.9.2	Piezoelectric model	100
4.10	Summary	102
5	Conclusions and future work	103
	Appendices	106
A	Constitutive relations for magnetoelasticity	106
A.1	Saint Venant-Kirchhoff model	106
A.2	Compressible nonlinear material model	107
B	First derivatives of $\tilde{\Phi}$ with respect to $(\epsilon, \kappa, \beta, \zeta, \eta)$	109
C	Some results	113
C.1	To Prove: $[\boldsymbol{\tau}^{e*} - \boldsymbol{\tau}^e] \mathbf{n} = \gamma_f^s \mathbf{E} + \frac{(\gamma^s)^2}{2\epsilon_0} \mathbf{n}$	113
C.2	Gauss divergence theorem to transform a surface integral to a volume integral	113
D	Surface integrating factor and surface normal	115
E	Constitutive relations for electroelasticity	117
	Bibliography	119

List of Figures

1.1	Schematic representation of diamagnetic, paramagnetic, and ferromagnetic materials microscopic structure in the presence of an applied magnetic field \mathbf{H}_a	5
2.1	A typical magnetoelastic body \mathcal{B}_0 (shaded) undergoing deformation: the underformed free space is denoted by \mathcal{B}_0^* while its outer boundary $\partial\mathcal{B}^\infty$ is assumed to remain unchanged during deformation.	9
2.2	A typical helically anisotropic magnetoelastomeric tube: green lines denote the direction of preferred magnetization.	11
2.3	A typical cross section of a tube, with inner radius R_1 , outer radius R_2 , wire radius r_δ and free space boundary radius r_∞	13
2.4	Regions of negative Poisson's effect: the region with solid red line boundary corresponds to torsionally relaxed case while the region having dashed black line boundary corresponds to torsionally constrained case ($\bar{\lambda} = 0.5$, $\nu_{iso} = 0.1$, $\nu_{21} = 0.1$) (a) $\zeta^* = 0$, $\eta^* = 0$ (b) $\zeta^* = 0.1$, $\eta^* = 0$ (c) $\zeta^* = 0$, $\eta^* = 0.1$	22
2.5	Effect of magnetic field on overwinding/unwinding characteristic in tubes having $\nu_{iso} = -0.345$, $\nu_{21} = -0.3$ (shaded region corresponds to overwinding) (a) $\zeta^* = 0$, $\eta^* = 0$ (b) $\zeta^* = 0.05$, $\eta^* = 0$ (c) $\zeta^* = 0$, $\eta^* = 0.15$	24
2.6	Effect of magnetic field on overwinding/unwinding characteristic for elastically isotropic tubes (shaded region corresponds to overwinding) (a) $\zeta^* = 0.05$, $\eta^* = 0$ (b) $\zeta^* = 0$, $\eta^* = 0.05$	25
2.7	Non-dimensionalized difference in total surface traction at the inner and outer radii vs. imposed inflation for incompressible and isotropic thick magnetoelastic tubes ($\zeta = 1.5$ kA, $\eta = 0$ kA/m, $\epsilon = -0.1$, $\kappa = 0$, $R_2/R_1 = 1.3$).	26
2.8	Non-dimensionalized internal pressure vs. imposed inflation in thin tubes at ($\epsilon = 0$, $\kappa = 0$) having $\alpha = 0^\circ$, $\nu = 0.3$	27
2.9	Induced inflation vs. imposed axial strain in torsionally relaxed compressible Mooney-Rivlin tubes, with solid and dotted lines corresponding to $\alpha = 0^\circ$ and $\alpha = 30^\circ$ respectively ($\nu = -0.1$).	28
2.10	Extension-torsion coupling in tubes having $\nu = 0.3$, $\alpha = 10^\circ$	28
2.11	Extension-torsion coupling in tubes having $\nu = 0.3$, $\alpha = 70^\circ$	29
3.1	A typical rod deforming from its straight state reference configuration.	31

3.2	A magnetoelastic rod embedded with magnetizable spheroidal inclusions: the inclusions are all assumed to be aligned along an arbitrary direction \mathbf{a} (typically along the rod's undeformed axis) in the rod's reference configuration	33
3.3	The case of magnetic field \mathbf{H}_a and undeformed inclusion \mathbf{a} being perpendicular to each other: $\hat{\mathbf{z}}$ equals $\mathbf{a} \times \mathbf{H}_a$ while the shaded plane is the plane containing $\hat{\mathbf{z}}$ and \mathbf{e}_3	40
3.4	Buckling curves for a clamped-free rod under combined compressive axial load and magnetic field acting perpendicular to undeformed inclusion orientation ($\lambda = 1.5$ corresponding to incompressible material)	49
3.5	Buckling curves for a clamped-clamped rod under combined compressive axial load and magnetic field acting perpendicular to undeformed inclusion orientation ($\lambda = 1.5$ corresponding to incompressible material)	49
3.6	Buckling curves for a clamped-pinned rod under pure magnetic loading acting perpendicular to the undeformed inclusion orientation	50
3.7	The case of applied magnetic field and undeformed inclusion orientation being parallel to each other	50
3.8	Buckling curves for a clamped-clamped rod under combined axial compressive load and magnetic field acting parallel to undeformed inclusion orientation ($\lambda = 1.5$ corresponding to incompressible material).	54
3.9	Buckling surface for the combined loading of magnetic field, axial load and twisting moment with undeformed inclusions oriented parallel to the rod axis and magnetic field perpendicular to it: the intersection of the surface in the three coordinate planes are also shown along with the stable region	58
3.10	Buckling curves for combined magnetic field and twisting moment with undeformed inclusions parallel to the rod axis and magnetic field perpendicular to it.	60
3.11	Buckling curves for the case of combined magnetic field, compressive load and twisting moment with undeformed inclusions and magnetic field both parallel to the rod axis	62
3.12	Buckling surface for the combined loading of magnetic field, axial load and twisting moment with undeformed inclusions oriented perpendicular to the rod's axis and magnetic field parallel to the rod's axis: the intersection of the surface in the three coordinate planes are also shown along with the stable region.	63
4.1	A typical electroelastomeric body \mathcal{B}_0 (shaded) undergoing deformation: the undeformed free space is denoted by \mathcal{B}_0^* while its outer boundary $\partial\mathcal{B}^\infty$ is assumed to remain unchanged during deformation.	68
4.2	Figure showing a tiny patch of an arbitrary surface having total surface charge density γ^s	72
4.3	Figure showing free body diagram of a rod's segment.	73
4.4	Geometric representation of a slender body of length $2l$ and maximum radius r_f	79
4.5	Schematic of an electroelastic rod with a load and a constant potential at one of its end.	97

4.6	Transverse displacement vs load plot for an electroelastic rod having $Y = 200\text{KPa}$, $G = 80\text{KPa}$, $l = 10\mu\text{m}$, $\epsilon = 0.01$, $\bar{\phi}(\bar{s} = -1) = 0$, $\bar{\phi}(\bar{s} = 1) = 5$, $\hat{p} = 0$	97
4.7	Transverse displacement vs load plot for an electroelastic rod having $Y = 200\text{KPa}$, $G = 80\text{KPa}$, $l = 10\mu\text{m}$, $\epsilon = 0.01$, $\bar{\phi}(\bar{s} = -1) = 0$, $\bar{\phi}(\bar{s} = 1) = 5$, $\hat{p} = 0.05$	98
4.8	Schematic of an electroelastic rod with a moment and a constant potential at one of its end.	98
4.9	Transverse displacement vs moment plot for an electroelastic rod having $Y = 200\text{KPa}$, $G = 80\text{KPa}$, $l = 10\mu\text{m}$, $\epsilon = 0.01$, $\bar{\phi}(\bar{s} = -1) = 0$, $\bar{\phi}(\bar{s} = 1) = 5$, $\hat{p} = 0$	99
4.10	Transverse displacement vs moment plot for an electroelastic rod having $Y = 200\text{KPa}$, $G = 80\text{KPa}$, $l = 10\mu\text{m}$, $\epsilon = 0.01$, $\bar{\phi}(\bar{s} = -1) = 0$, $\bar{\phi}(\bar{s} = 1) = 5$, $\hat{p} = 0.05$	99
4.11	Transverse displacement vs load plot for a piezoelectric rod poled along \mathbf{e}_3 direction having $Y = 126\text{GPa}$, $G = 48\text{GPa}$, $l = 10\mu\text{m}$, $\epsilon = 0.01$, $\mathcal{E}_{3,33}^0 = 23.3\text{C/m}^2$ (a) $\bar{\phi}(\bar{s} = 1) = 1.2$ (b) $\bar{\phi}(\bar{s} = 1) = 2$	100
4.12	Transverse displacement vs moment plot for a piezoelectric rod poled along \mathbf{e}_3 direction having $Y = 126\text{GPa}$, $G = 48\text{GPa}$, $l = 10\mu\text{m}$, $\epsilon = 0.01$, $\mathcal{E}_{3,33}^0 = 23.3\text{C/m}^2$ (a) $\bar{\phi}(\bar{s} = 1) = 1.0$ (b) $\bar{\phi}(\bar{s} = 1) = 2$	101

List of Tables

2.1	Piezomagnetic coupling constants for Cobalt Ferrite ($CoFe_2O_4$).	23
3.1	Buckling equations for the case of combined magnetic field and compressive axial loading with magnetic field perpendicular to undeformed inclusion orientation: the expressions in blue are the modes which are unaffected by the presence of magnetic field and hence also arise in purely elastic case .	46
3.2	Buckling equations for the case of combined magnetic field and axial compressive loading case with magnetic field perpendicular to undeformed inclusion orientation	47
3.3	Buckling equations for the case of pure magnetic loading with magnetic field perpendicular to undeformed inclusion orientation	48
3.4	Buckling equations for the case of combined magnetic field and compressive axial loading with magnetic field parallel to undeformed inclusion orientation	52
3.5	Buckling equations for the case of combined magnetic field and axial compressive loading with magnetic field parallel to undeformed inclusion orientation	52
4.1	Exact values of the integrals in equation (4.84) for different values of i and j .	88
4.2	Asymptotic values of the integrals in equation (4.84) for different values of i and j	89
4.3	Expressions of different quantities appearing in governing equations . . .	92
4.4	Constitutive equations for a specific nonlinear electroelastic material model discussed in Appendix E	92
E.1	Piezoelectric constants for PZT-5H when poled along \mathbf{e}_1 direction	118
E.2	Piezoelectric coupling constants for PZT-5H when poled along \mathbf{e}_2 direction.	118
E.3	Piezoelectric coupling constants for PZT-5H when poled along \mathbf{e}_3	119